Zoodiversity, 59(5): 477–492, 2025

DOI 10.15407/zoo2025.05.477
UDC 595.768.11:57.087.1:577.21

WHEN MORPHOLOGY MEETS MOLECULES: BARCODING CONFIRMS AN ANCIENT SEPARATION OF *PHYTOECIA TIGRINA* SUBSPECIES (COLEOPTERA, CERAMBYCIDAE)

A. M. Zamoroka

Vasyl Stefanyk Precarpathian National University,
Taras Shevchenko St., 57, Ivano-Frankivsk, 76018 Ukraine

E-mail: andrew.zamoroka@pnu.edu.ua

https://orcid.org/0000-0001-5692-7997

urn:lsid:zoobank.org:pub:D6FD470B-AF17-4E03-BEC2-E27B72BEC526

When Morphology Meets Molecules: Barcoding Confirms an Ancient Separation of *Phytoecia tigrina* subspecies (Coleoptera, Cerambycidae). Zamoroka, A. M. — The molecular analysis of *Phytoecia tigrina* revealed substantial genetic differentiation (5.8–7.0%) between populations on opposite sides of the Carpathian Arc. Two distinct haplogroups were identified: PhtZk (western, haplotype PhtZk-1) and PhtPo (eastern, haplotypes PhtPo-1 and PhtPo-2), including the type locality of *Phytoecia tigrina podillica* Zamoroka, Ruicănescu & Manci, 2024. These findings support the division of *Ph. tigrina* into two subspecies. The pronounced genetic divergence suggests that the separation between *Ph. tigrina tigrina* and *Ph. tigrina podillica*, occurred much earlier than previously assumed. Moreover, the coexistence of two highly distinct haplotypes within *Ph. tigrina podillica* populations suggests episodes of rapid range expansions and contractions during the Late Pleistocene and Holocene. Overall, our results provide valuable insights into the evolutionary processes driving intraspecific diversification in *Ph. tigrina* in response to cyclical climate fluctuations.

Key words: longhorn beetles, barcoding, molecular phylogeny, speciation, evolution, metapopulations, range dynamics, climate changes.

Introduction

Phytoecia (*Pilemia*) *tigrina* (Mulsant, 1851) is a Ponto-Pannonian subendemic species, distributed in Europe across the Danube and Dnister River basins, as well as the Balkan Mountains (Zamoroka et al., 2024). Its range includes Hungary, Ukraine, Romania, Moldova, Serbia, Bulgaria, and western Turkey (Crișan et al., 2017; Zamoroka et al., 2024). This species is among very few

longhorn beetles (Cerambycidae) strictly protected under various European legal frameworks. These include the EU Habitats Directive (Council Directive, 1992; Crișan et al., 2017), Resolution 6 of the Convention on the Conservation of European Wildlife and Natural Habitats (Bern Convention) (Revised Annex I…, 2011; Crișan et al., 2017; Zamoroka et al., 2024), and the Red Data Book of Ukraine (Zamoroka, 2022 a, b; Zamoroka et al., 2024).

The conservation status of *Ph. tigrina* has long been associated with its low population density, the patchy distribution of its host plant, *Cynoglottis barrelieri* (All.) Vural& Kit Tan, and the extreme fragmentation of its habitat (Crișan et al., 2017; Zamoroka et al., 2024). Despite the host plant's extensive range in Europe and Asia Minor, the range of *Ph. tigrina* is significantly smaller, primarily limited by the availability of suitable ecological conditions (Zamoroka et al., 2024). The species is confined to thermophilous habitats, specifically calcareous steppe meadows and dry grasslands on loess or rocky substrates where its host plant occurs (Report… 2013–2018).

Over the past decade, several studies have focused on the population status of *Ph. tigrina*, reporting new localities and providing data that have considerably expanded knowledge of its range, biology, and ecology (Ilić & Ćurčić, 2015; Tóth et al., 2016; Crișan et al., 2017; Tezcan et al., 2020; Bacal et al., 2020; Georgiev, 2020; Zamoroka, 2022 c; 2023; Zamoroka et al., 2024). The recent surge in research attention is likely driven by the species' conservation status and the need to assess its populations for the development and implementation of conservation management plans. This need arises largely from the lack of comprehensive information available in standard datasets such as Natura 2000 and EUNIS. Unfortunately, despite the significant amount of recent data on the distribution, biology, and ecology of *Ph. tigrina*, these datasets remain outdated and provide limited information.

Our recent study (Zamoroka et al., 2024) has provided comprehensive information on the distribution, ecology, and evolution of *Ph. tigrina*. At the same time, significant morphological differences were identified between metapopulations of *Ph. tigrina* located east and west of the Carpathian Arc. These findings served as the basis for the taxonomic division of the species into two subspecies: *Phytoecia* (*Pilemia*) *tigrina tigrina* (Mulsant, 1851) and *Ph.* (*P.*) *tigrina podillica* Zamoroka, Ruicănescu & Manci, 2024. A key focus of the study was the differentiation of *Ph. tigrina* metapopulations on either side of the Carpathian Arc during the Holocene, followed by their divergence and the emergence of new morphological traits (Zamoroka et al., 2024). Morphological differences, combined with ecological niche modeling based on paleoclimatic data, allowed for a broad reconstruction of the species' evolutionary history and the identification of the most likely glacial refugia of *Ph. tigrina* in Europe. However, a limitation of that study was the reliance solely on morphological traits, as molecular data were not available at the time. As a result, the findings provide only a partial understanding of the evolutional processes that shaped *Ph. tigrina* metapopulations.

In the current study, we conducted the first sequencing of a 658-nucleotide fragment (the standard DNA barcode) of the cytochrome c oxidase subunit I gene (COI) for *Ph. tigrina.* The main objective of this study is to test the validity of dividing *Ph. tigrina* into two subspecies using molecular phylogenetic methods. Additionally, we aimed to estimate the divergence time of these subspecies using a molecular clock approach.

Material and Methods

Specimens of *Ph. tigrina* were collected during April–May 2018–2020 from the Zakarpattia and Ivano-Frankivsk Regions of Ukraine (Fig. 1; Table 1). For genetic analysis, only the right hind leg of adult specimens was preserved in 96% ethanol under field conditions, properly labeled, and transported to the laboratory. Before DNA extraction, the samples were stored in ethanol at –20 °C to ensure DNA integrity. Vouchers (adult specimens, which are the DNA donors) have been deposited in the entomological collection of Vasyl Stefanyk Precarpathian National University, Ivano-Frankivsl, Ukraine (PUIF).

DNA Extraction. The femur muscles of *Ph. tigrina* were used for DNA extraction. The femur was cut into small pieces using sterile microscissors and placed in an individual well of a 96-well PCR plate. A total of 25 μL of lysis buffer C was added to each sample, consisting of 200 mM Tris (pH 8.0), 25 mM EDTA (pH 8.0), 0.05% Tween-20, and 0.4 mg/ml Proteinase K

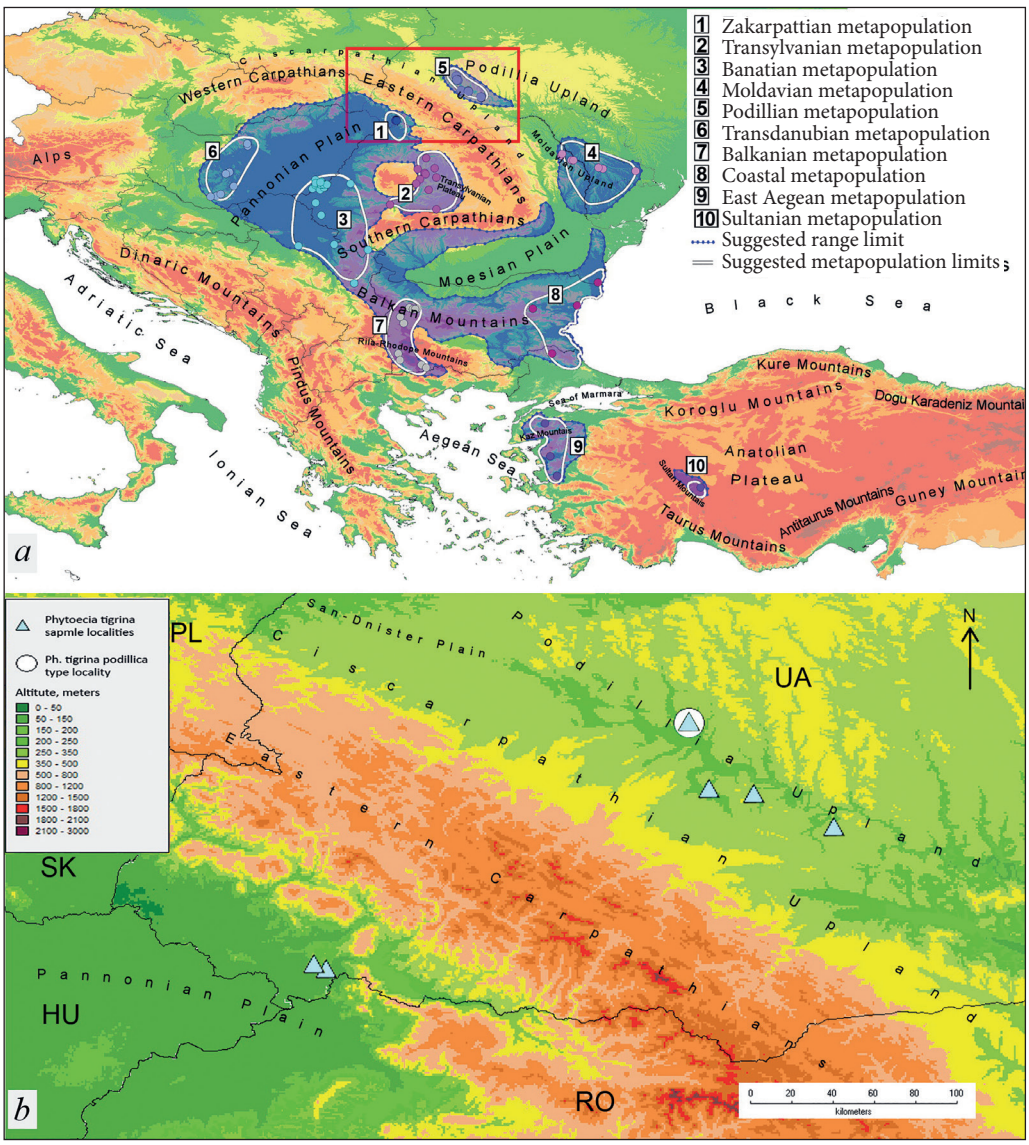

Fig. 1. General distribution range of *Phytoecia tigrina* (adapted from Zamoroka et al., 2024) (*a*), with the barcode sampling area highlighted (*b*)

(Korlević et al., 2021). The mixture was homogenized to ensure even distribution of the lysis buffer, followed by incubation at 56 °C for two hours to facilitate complete cell lysis and DNA release. After incubation, a portion of the lysate was diluted 10-fold, and subsequent PCR steps were carried out using the unpurified DNA extract (Korlević et al., 2021; Makunin et al., 2022).

PCR. Indexed universal COI primers HCO and LCO were used for PCR amplification (Srivathsan et al., 2021). The reaction mix was prepared as follows: 5 μL of Master Mix (MM), 0.3 μL of Forward Primer (Pr F), 0.3 μL of Reverse Primer (Pr R), 3.2 μL of distilled water, 0.7 μL of DNA template, and 0.5 μL of Dimethyl sulfoxide (DMSO), resulting in a final volume of 10 μL per reaction. The PCR conditions included an initial denaturation at 95 °C for 2 minutes, followed by 25–35 cycles of denaturation at 95 °C for 30 seconds, annealing at 40 °C for 30 seconds, and extension at 72 °C for 45 seconds. A final extension at 72 °C for 5 minutes was performed to complete amplification. A 2 μL aliquot of each PCR product was immediately analyzed via gel electrophoresis for DNA verification, while the remaining volume was stored at 4 °C for subsequent sequencing.

Table 1. **The COI sequences used in the current study**

Species	Isolate (this study)	GenBank voucher	Boldsystems voucher
Phytoecia tigrina tigrina	CER-107	PV408207	–
Phytoecia tigrina tigrina	CER-108	PV408206	–
Phytoecia tigrina podillica	CER-172	PV408208	–
Phytoecia tigrina podillica	CER-173	PV408209	–
*Phytoecia tigrina podillica**	CER-187	PV408210	–
Phytoecia tigrina podillica	CER-188	PV408211	–
Phytoecia affinis	CER-94	PV655108	–
Phytoecia affinis	CER-95	PV655109	–
Phytoecia affinis	CER-96	PV655110	–
Phytoecia affinis	CER-182	PV655113	–
Phytoecia affinis	–	–	GBCLC1882-19
Phytoecia affinis	–	–	GBCLC1883-19
Phytoecia pustulata	CER-181	PV655112	–
Phytoecia pustulata	–	–	GBCOU5162-14
Phytoecia pustulata	–	–	TDAOE1874-23
Phytoecia pustulata	–	–	GBAAW53195-24
Phytoecia pustulata	–	–	GCOL11363-16
Phytoecia pustulata	–	–	GCOL4268-16
Phytoecia virgula	CER-106	PV655114	–
Phytoecia virgula	–	–	GBMUS006-17
Phytoecia virgula	–	–	GBMUS007-17
Phytoecia virgula	–	–	TDAAT153-19
Phytoecia caerulea	CER-98	PV655111	–
Phytoecia caerulea	–	–	UNIFI975-24
Phytoecia caerulea	–	–	UNIFI977-24
Phytoecia cylindrica	CER-179	PV655115	–
Phytoecia cylindrica	–	–	GBCOU1126-13
Phytoecia cylindrica	–	–	FBCOA539-10
Phytoecia cylindrica	–	–	DTNHM6394-23
Phytoecia cylindrica	–	–	UKAN3660-24
Phytoecia cylindrica	–	–	NOCLP2082-20
Phytoecia caerulescens	–	–	CLPFR020-21
Phytoecia caerulescens	–	–	GCOL11827-16
Phytoecia caerulescens	–	–	GRAEL1390-22
Phytoecia caerulescens	–	–	TDAOE3501-23
Phytoeciauncinata	–	–	GBCOU5164-16
Phytoeciauncinata	–	–	GBCOU9570-15
Oberea linearis	–	KU917689.1	–
Oberea oculata	–	HQ559268.1	–
Saperda scalaris	CER-123	PV655116	–
Menesia bipunctata	CER-208	PV655117	–

* Sequence from the type locality of *Phytoecia tigrina podillica.*

Library Preparation and Sequencing. The DNA barcoding workflow was followed for sequencing (Srivathsan et al., 2021). The process began with barcode attachment, where uniquely indexed primers were used during PCR amplification to generate distinguishable sequence tags for each sample. After amplification, PCR products were pooled together, ensuring an even distribution of each sample within the sequencing library. For library preparation, the pooled PCR amplicons were purified using a magnetic bead-based cleanup step to remove excess primers, nucleotides, and other reaction components that could interfere with sequencing. The purified amplicons were then ligated with ONT sequencing adapters using the ligation sequencing kit, allowing compatibility with the ONT flow cell. The prepared library was quantified to assess DNA concentration and quality before loading onto the sequencing platform. During sequencing, the prepared library was introduced into the ONT flow cell and processed using a MinION device. The sequencing run was monitored in real-time to ensure high-quality data acquisition. Once sequencing was complete, base calling was performed to convert raw signal data into nucleotide sequences. Subsequent bioinformatics processing included demultiplexing the barcoded reads, filtering for high-quality sequences, and generating consensus sequences. These steps were conducted using ONTBarcoder 2.0 (Srivathsan et al., 2024) to ensure accurate sequence reconstruction and species identification.

Phylogenetic Analysis. The phylogenetic analysis was performed using Seaview 5.0, a multi-platform software designed for sequence alignment, molecular phylogenetics, and tree reconciliation (Gouy et al., 2021). Multiple sequence alignments were generated with the MUSCLE algorithm integrated within Seaview 5.0. The resulting alignments were reviewed and manually refined to correct regions with missing data and eliminate poorly aligned positions. Phylogenetic trees were constructed using the maximum likelihood (ML) method implemented in the PhyML algorithm (Guindon et al., 2010). The general time-reversible (GTR) model was selected to describe sequence evolution, while branch support was evaluated through the approximate likelihood-ratio test (aLRT), which compares the log-likelihood values of the inferred tree and alternative topologies (Anisimova & Gascuel, 2006; Guindon et al., 2010). Tree topology optimization was conducted using a combination of nearest-neighbor interchange (NNI) and subtree pruning and regrafting (SPR) strategies. Additionally, the neighbor-joining (BioNJ) algorithm was applied to enhance branch length estimation and improve the overall tree structure (Gascuel, 1997). The Jukes-Cantor (1969) genetic distance model was used for the calculation of the genetic distances.

Estimation of molecular divergence and evolution. To estimate the species tree, a Nexus file containing 41 sequences of 658-nucleotide fragments of the COI gene was prepared and loaded into BEAST2 v2.7.5 (Bouckaert et al., 2019) using the BEAUti interface. The analysis was conducted under the Yule speciation process (Gernhard, 2008), a model that assumes a constant rate of speciation across lineages, making it suitable for species-level phylogenetics. An uncorrelated relaxed clock with a lognormal distribution (Drummond et al., 2006) was applied to account for variation in mutation rates among lineages, allowing the model to estimate different rates for different branches without assuming strict uniformity. A Bayesian Markov chain Monte Carlo (MCMC) analysis was run for 10 million generations, with sampling performed every 1000 steps to ensure comprehensive exploration of tree space. After completion, Tracer v1.7.2 (Rambaut et al., 2018) was used to assess the convergence of the MCMC runs by evaluating the effective sample sizes (ESSs) of estimated parameters, ensuring that they were sufficiently large to support reliable inferences. To obtain a final consensus tree, multiple independent runs were combined using LogCombiner v2.7, which merged posterior distributions while discarding a portion of early samples as burn-in to remove artifacts of initial model adjustments. A maximum clade credibility (MCC) tree representing the best-supported topology was generated using TreeAnnotator v2.7.5, which calculates posterior probabilities for each clade based on the sampled trees (Bouckaert et al., 2019). The resulting MCC tree was visualized and annotated in FigTree v1.4.4 (Rambaut, 2014), a software designed for graphical representation of phylogenetic trees, allowing for further interpretation and analysis of evolutionary relationships.

Nodes calibration. The calibration of the tree nodes was based on fossil data for representatives of the genus *Saperda*. This approach was necessary because no fossil remains are known for *Phytoecia*, and those attributed to *Oberea* are highly questionable (e. g., *Oberea praemortua* von Heyden, 1862 is known from a single elytron). Nevertheless, *Saperda* is well documented in the fossil records from the Late Miocene (e. g., *Saperda florissantensis* Wickham, 1916) and Plio-

cene (e. g., *Saperda robusta* (Schmidt, 1967)) (Vitali, 2015). Many other species previously interpreted as *Saperda*, as noted by Vitali (2015), do not actually belong to this genus. Although the oldest representative of *Saperda* is considered to be *Saperda caroli* Vitali, 2015 from the Early Eocene, it is likely that this species also does not belong directly to *Saperda*, but rather represents one of the basal groups of the tribe *Saperdini*. Therefore, for calibration in this study, an average divergence time between the *Saperda–Menesia* and *Oberea–Phytoecia* lineages in the Middle Miocene (11 Ma) was adopted.

Results

Resultantly, we obtained for the first time 658-nucleotide sequences of the cytochrome c oxidase subunit I (COI) gene (the standard DNA barcode) for *Ph. tigrina*. This allowed us to perform a comparative phylogenetic analysis of specimens collected from the both sides of Carpathian Arc named Zakarpattian (west side) and Podillian (east side) metapopulations (for details see Zamoroka et al., 2024). Our findings reveal significant genetic differences between the analyzed samples from both metapopulations, ranging from 5.8% to 7.0%. In contrast, genetic variability within each metapopulation is substantially lower: 0.0–0.9% for the Zakarpattian metapopulation and 0.0–3.7% for the Podillian metapopulation (Table 2).

Our results allowed us to identify two haplogroups, each corresponding to one of the studied metapopulations. Specifically, haplogroup *PhtZk* is characteristic of the Zakarpattian metapopulation, while haplogroup *PhtPo* is associated with the Podillian metapopulation. Within haplogroup *PhtZk*, we identified only one haplotype — *PhtZk-1*. In contrast, haplogroup *PhtPo* contains two distinct haplotypes: *PhtPo-1* (including the topogenotype COI of *Ph. t. podillica*) and *PhtPo-2*.

To facilitate comparison, we constructed a consensus sequence as a reference and examined three haplotypes to determine key nucleotide substitutions (Fig. 2). These substitutions serve as clear genetic markers for haplotype identification. Haplotype *PhtPo-1* is characterized by seven key nucleotide substitutions; haplotype

Table 2. **Pairwise comparison of nucleotide sequences within *Ph. t. tigrina* and *Ph. t. podillica*: upper right — percentage (%) differences; lower left — genetic distances (substitutions per site)**

Isolate	*Ph. t. tigrine* CER-107	*Ph. t. tigrine* CER-108	*Ph. t. podillica* CER-172	*Ph. t. podillica* CER-173	**Ph. t. podillica* CER-187	*Ph. t. podillica* CER-188
Ph. t. tigrina CER-107	0.0	0.9	7.0	6.3	5.8	5.8
Ph. t. tigrina CER-108	0.009	0.0	7.0	6.3	5.8	5.8
Ph. t. podillica CER-172	0.072	0.072	0.0	3.7	3.3	3.3
Ph. t. podillica CER-173	0.063	0.063	0.039	0.0	0.5	0.5
**Ph. t. podillica* CER-187	0.058	0.058	0.034	0.004	0.0	0.0
Ph. t. podillica CER-188	0.058	0.058	0.034	0.004	0.000	0.0

* Sequence from the type locality of *Phytoecia tigrina podillica*

PhtPo-2 exhibits 14 substitutions and finally haplotype *PhtZk-1* is the most distinct, with 33 substitutions.

Our analysis demonstrates that each haplotype possesses a unique set of nucleotide substitutions, reflecting long-standing divergence processes between and within the metapopulations they represent. Notably, haplotypes *PhtPo-1* and *PhtPo-2* differ by 3.3–3.7%, yet both occur within a relatively small geographic area and belong to the same metapopulation. This degree of genetic variation likely indicates a complex evolutionary history for the Podillian metapopulation, involving multiple migration waves and potential local extinctions throughout the Holocene.

The genetic variability among the identified haplogroups and haplotypes of *Ph. t. tigrina* and *Ph. t. podillica*, as well as the outgroup species, is visualized in the phylogenetic tree (Fig. 3), which exhibits a high level of branch support (SH = 0.83–1.00). This tree clearly illustrates the deep divergence between the *Ph. tigrina* metapopulations located on opposite sides of the Carpathian Arc. Specimens from the Zakarpattian metapopulation (*Ph. t. tigrina*) form a single cluster representing haplogroup *PhtZk*, with intra-group variability reaching up to 0.9%. In contrast, specimens from the Podillian metapopulation (*Ph. t. podillica*) form a distinct and distant cluster corresponding to haplogroup *PhtPo*, which contains two haplotypes, *PhtPo-1* and *PhtPo-2*. The average genetic difference between these two haplotypes is 3.4%, while variation within each haplotype does not exceed 0.5%. Surprisingly, the average genetic distance between the two metapopulations reaches 6.2%. This significant genetic differentiation likely indicates a prolonged period of isolation between the *Ph. tigrina* metapopulations. Given the topology of our phylogenetic tree, we hypothesize that these results represent the final stages of speciation in geographically isolated populations of *Ph. tigrina*. A denser sampling of barcode sequences, including specimens from other metapopulations, is necessary to clarify the situation and make definitive conclusions regarding the taxonomic status of *Ph. t. tigrina* and *Ph. t. podillica*.

We estimated the probable divergence time (Fig. 4) of the three studied haplotypes of *Ph. tigrina* using COI molecular markers and the Calibrated Yule Model. Our results indicate that the average divergence time between *Ph. t. tigrina* and *Ph. t. podillica* is approximately ~1.2 Ma. The lower boundary of the divergence interval for these genetic lineages is estimated at ~1.7 Ma and the upper is ~0.7 Ma. Meanwhile, the average divergence time between haplotypes *PhtPo-1* and *PhtPo-2* within the Podillian metapopulation of *Ph. t. podillica* is approximately ~0.2 Ma, with relatively short range which is approximately ± 0.04 Ma. This time is two orders of magnitude greater than we previously assumed based solely on bioclimatic modelling of the ecological niche for *Ph. tigrina* (Zamoroka et al., 2024). Overall, the Mid-Pleistocene Transition (~1.25–0.7 Ma) should be considered the key period of divergence between the evolutionary lineages of *Ph. t. tigrina* and *Ph. t. podillica*. Furthermore, our current study, based on COI molecular markers, enhances our understanding of the range dynamics of *Ph. t. podillica*, revealing periods of its rapid expansion and contraction influenced by climatic oscillations during the Late Pleistocene. In light of these new molecular data, the results of bioclimatic modeling from our previous study should be reinterpreted.

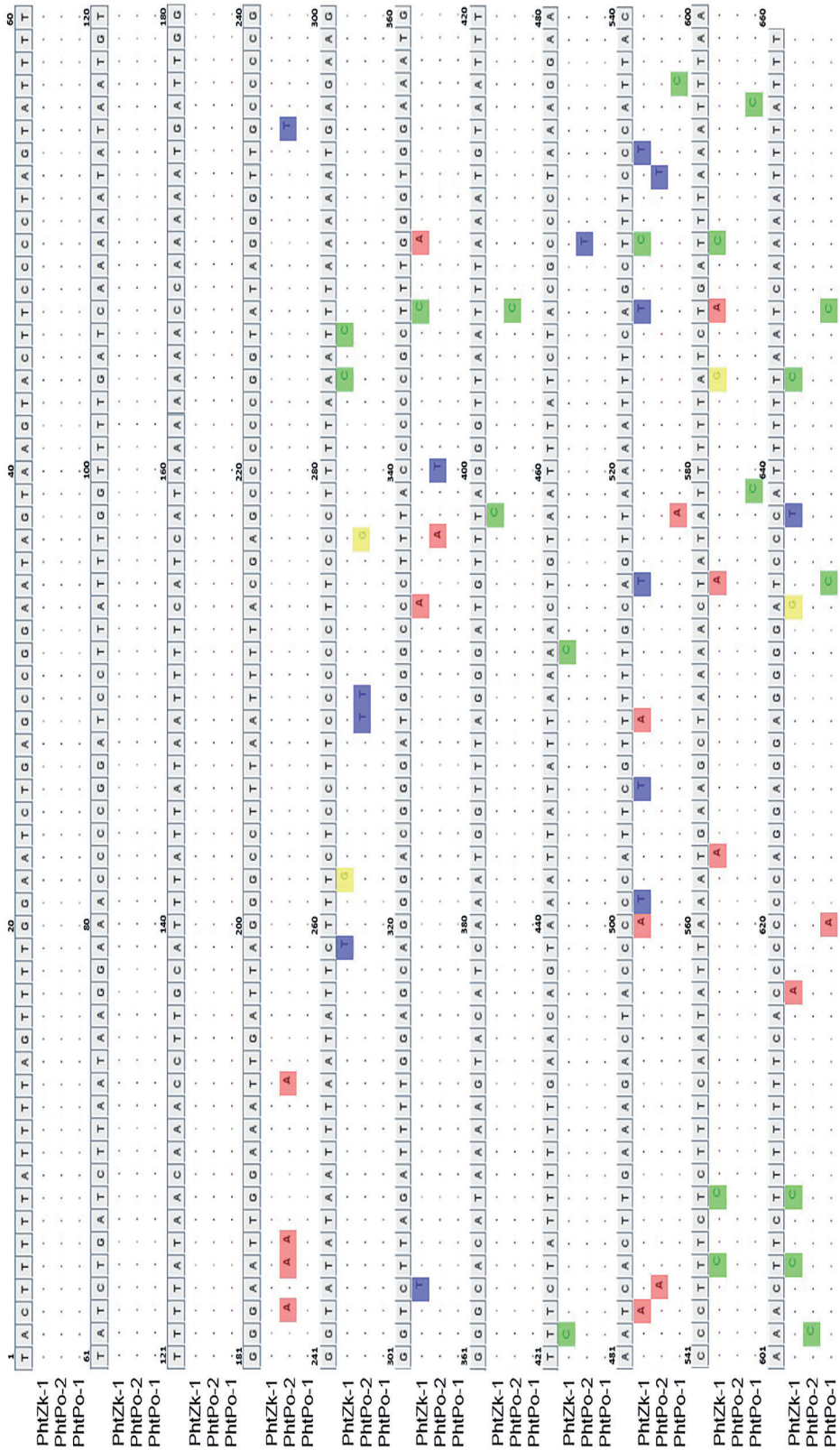

Fig. 2. Comparison of consensus sequences of haplotypes of *Phytoecia tigrina tigrina* (*PhtZk-1*) and *Ph. tigrina podillica* (*PhtPo-1* and *PhtPo-2*). Unique nucleotide substitutions for each haplotype are highlighted in colour

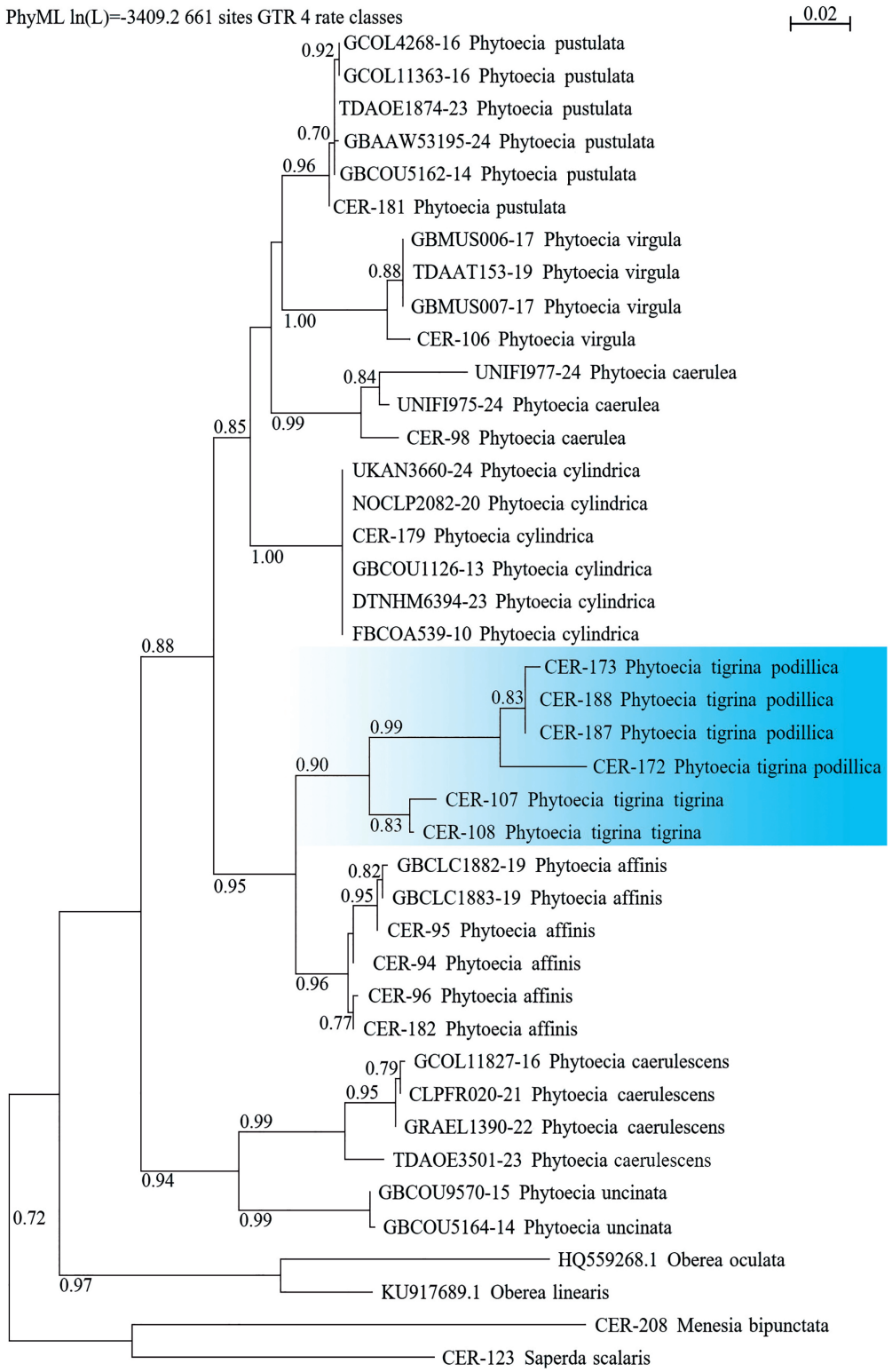

Fig. 3. Intraspecific phylogenetic relationships between *Phytoecia tigrina tigrina* and *Ph.tigrina podillica* (highlighted)

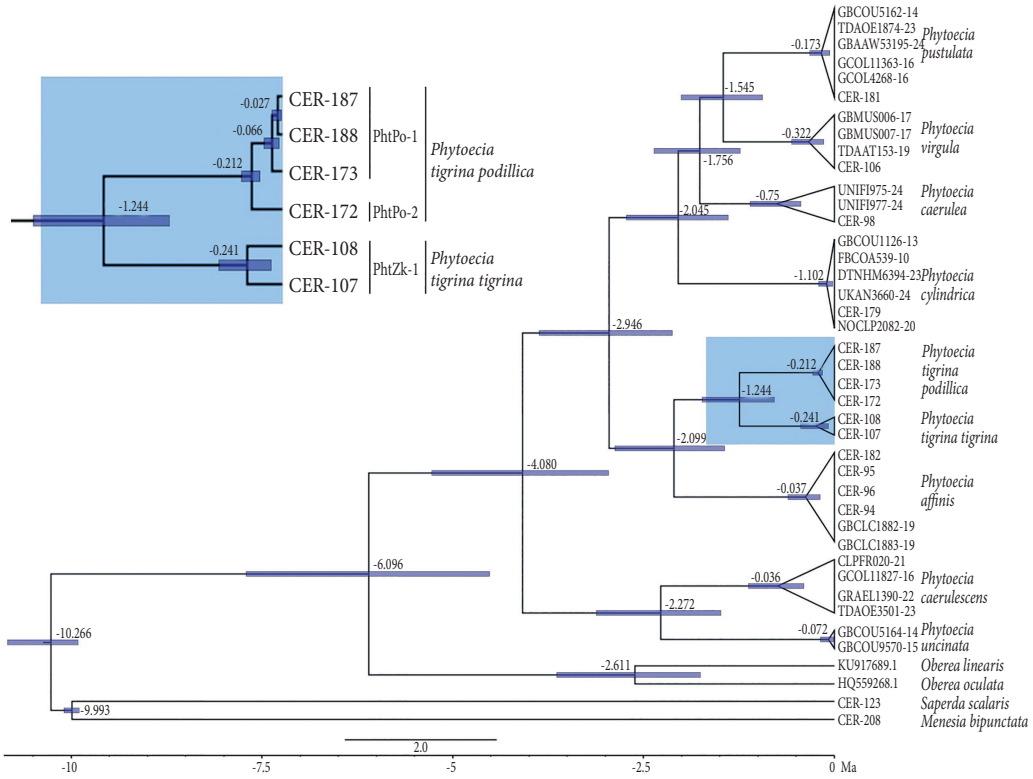

Fig. 4. Estimated divergence time between haplotypes of *Phytoecia tigrina tigrina* (*PhtZk-1*) and *Ph. tigrina podillica (PhtPo-1* and *PhtPo-2*) (highlighted); The mean node divergence time values are shown; Time scale is in millions of years (Ma)

Discussion

Our study presents the results of COI sequencing for *Ph. tigrina*, including materials from two metapopulations located to the east and west of the Carpathian Arc. These sequences represent the two subspecies, *Ph. t. tigrina* and *Ph. t. podillica*, whose subdivision we previously proposed based on morphological and ecological characteristics (Zamoroka et al., 2024). Our earlier research did not include molecular data; however, in this study, such data became available, confirming the validity of our previous conclusions regarding the differentiation of *Ph. tigrina* on two subspecies. Specifically, our molecular analysis revealed deep genetic differences between the two studied metapopulations. The dissimilarity between *Ph. tigrina* sequences from the Zakarpattian and Podillian metapopulations ranges from 5.8% to 7.0%. It is significantly higher than the 2.2–2.9% differences we previously observed when delimiting subspecies of *Anastrangalia dubia* (Scopoli, 1763) (Zamoroka et al., 2019). This suggests a more advanced stage of speciation than we have documented before.

The significant genetic differences between *Ph. t. tigrina* and *Ph. t. podillica* may be due to their location at the northernmost extremes of the *Ph. tigrina* range separated by Carpathian Arc. As a result, these metapopulations have experienced long-term isolation and strong divergence, both from each other and from other popula-

tions. Reveled previously (Zamoroka et al., 2024) distinct differences in morphology and structure of terminalia between *Ph. t. tigrina* and *Ph. t. podillica* in the Zakarpattian and Podillian metapopulations, along with currently found substantial genetic dissimilarities, suggest that speciation is in its final stages. In our previous study (Zamoroka et al., 2024), we found intermediate morphological traits of both subspecies in the Moldavian metapopulation. This may result from introgression between the two subspecies in the Southern Carpathians. Based on our findings, we suggest that gene flow occurs between neighboring metapopulations. However, whether a reproductive barrier exists between the most divergent of them remains unknown, as has been shown for many other biological species (Eckert et al., 2008; Hargreaves & Eckert, 2013; Turner, 2013). In this context, our research contributes to a growing body of studies that have explored various speciation mechanisms in cerambycid beetles using molecular phylogenetics, including hybridization, ecological diversification, reticulate evolution, convergence, and homoplasy (Zamoroka et al., 2019, 2022; Dascălu et al., 2021; Zamoroka, 2022 d; Karpiński et al., 2023, 2024; Caba & Dascălu, 2024).

The bioclimatic model presented in our previous study (Zamoroka et al., 2024) indicated that conditions suitable for the existence of *Ph. tigrina* east of the Carpathian Arc first emerged during the Preboreal time (10.3–9.0 ka) of the Pleistocene. This is significantly later than the divergence time estimated in the present study based on molecular data for *Ph. t. tigrina* and *Ph. t. podillica*, which averages around 1.2 Ma. This discrepancy can be explained by the fact that our earlier assessment considered bioclimatic suitability only for the late Pleistocene and Holocene, under the assumption that the Last Glacial Maximum acted as the primary trigger for the divergence of *Ph. t. tigrina* and *Ph. t. podillica*. However, this interpretation turned out to be incorrect, as both subspecies actually split much earlier, during the Middle Pleistocene.

Our molecular dating corresponds temporally with the Mid-Pleistocene Transition (~1.25–0.7 Ma), a period marked by significant climate cooling due to glacial stages that became at least twice as long (Scherrenberg et al., 2025). It is plausible that these prolonged glacial periods facilitated extended isolation of separate populations. It is likely that the genetic lineages of *Ph. t. tigrina* and *Ph. t. podillica* were already separated and well differentiated by this time, with divergence potentially beginning even before the onset of the Mid-Pleistocene Transition. This is further supported by the lower bound of the molecular time interval (1.7 Ma) indicated by our data (Fig. 4). The dynamics of the initial range of *Ph. tigrina* during this period remain unclear. However, it is likely that its distribution underwent repeated contractions and expansions corresponding to the alternating glacial and interglacial phases throughout the Middle and Late Pleistocene. Nevertheless, our results clearly indicate that ancestral populations persisted for an extended time on both sides of the Carpathian Arc.

Despite this, the question of the specific refugium from which the genetic lineage of *Ph. t. podillica* originated remains unresolved. The bioclimatic model we previously constructed (Zamoroka et al., 2024) reflects the probable range dynamics of *Ph. tigrina* at the end of the Pleistocene and throughout the Holo-

cene. According to this model, two main refugia for *Ph. tigrina* existed during the Last Glacial Maximum: one in the Pannonian Basin and another in the region of the Aegean and Marmara Seas. Additionally, scattered microrefugia likely persisted along the Danube Valley between the Black Sea and the Southern Carpathians. However, the molecular data obtained in this study point to a much earlier divergence of *Ph. t. tigrina* and *Ph. t. podillica* and a long-term isolation of their lineages. It is therefore plausible that ancient glacial microrefugia of *Ph. t. podillica* also existed in the Dnister Valley. This scenario appears particularly credible in light of the hypothesis proposed by Kajtoch et al. (2016), suggesting the existence of scattered microsite refugia for thermophilic biota in xerocryosteppe conditions within the periglacial zone during the last glaciation. Our current results may serve as indirect support for this hypothesis, though further studies are needed to confirm it.

A surprising result of our current study was the discovery of genetically distinct individuals within the Podillian metapopulation of *Ph. t. podillica*. Notably, the sample CER-172 from the Pidpechery population differs by 3.3–3.7% in the nucleotide sequence of the COI gene from the specimens collected in neighboring localities. This contrasts sharply with the other three populations, where genetic differences range from only 0.0% to 0.5%. This finding indicates that at least two distinct genetic lineages exist within the Podillian metapopulation, which we have identified as haplotypes *PhtPo-1* and *PhtPo-2*. This discovery likely represents a relic signal from the past, pointing to historical fluctuations in the range of *Ph. t. podillica*. We hypothesize that there were at least two waves of range expansion for *Ph. t. podillica*, separated by a period of significant contraction.

The estimated average divergence time between haplotypes *PhtPo-1* and *PhtPo-2* within the Podillian metapopulation of the subspecies *Ph. t. podillica* is approximately 0.2 Ma (Fig. 4). This event is likely associated with a substantial range contraction of *Ph. t. podillica* during the Riss glaciation (0.30–0.13 Ma). This contraction led to the formation of isolated populations east of the Carpathian Arc, although the exact locations of these refugia remain entirely unknown. It is probable that this range reduction caused a bottleneck effect, preserving only one or a few very small isolated populations of the *PhtPo-2* haplotype. At least one such population persisted in the western part of the Podillia Upland to the present day.

The expansion of the *PhtPo-1* haplotype, which is the most widespread among the studied populations, is associated with the end of the Würm glaciation, around 0.01 Ma. The origin of this expansion remains uncertain. It may have arisen from a small group of populations on the west of Podillia Upland or from a rapid and short-term migration from the Moldavian Plateau. Further detailed molecular studies across the entire range of *Ph. tigrina* are needed to clarify this question. Nevertheless, since mitogenomes are non-recombinant, both haplotypes *PhtPo-1* and *PhtPo-2* are maintained within the populations, despite introgression and hybridization between these two genetic lineages.

Conclusions

In summary, it should be emphasised that our current molecular phylogeny results fully support the validity of the previous division of *Ph. tigrina* into subspecies *Ph. t. tigrina* and *Ph. t. podillica*, based solely on morphological and ecological analysis. However, the divergence of the evolutionary branches of both subspecies is much more ancient as previously assumed, dating back to a time of the Mid-Pleistocene Transition. Climatic oscillations throughout the Late Pleistocene have also had a significant impact on the genetic structure of *Ph. t. podillica* populations, reflecting the complex history of its range expansion and contraction. Further research, including a significantly larger number of samples from all known metapopulations of *Ph. tigrina*, will address questions concerning the taxonomy, evolutionary history, and the impact of climate on this rare and protected the longhorn beetle.

Acknowledgements

I would like to express my sincere gratitude to Dr. Oleksandr Zinenko (V. N. Karazin Kharkiv National University, Kharkiv, Ukraine) for his invaluable contribution to the molecular studies presented in this research. I am also very grateful to Dr. Taras Yanytskyi, Director of the State Museum of Natural History of the NAS of Ukraine (Lviv, Ukraine), for providing free and unlimited access to the relevant laboratories. This study was conducted as part of the ongoing scientific research project titled "Molecular phylogeny and systematics of living organisms" (state registration number 0121U109305) at Vasyl Stefanyk Precarpathian National University.

REFERENCES

Anisimova, M. & Gascuel, O. 2006. Approximate likelihood ratio test for branches: A fast, accurate and powerful alternative. *Systematic Biology*, **55** (4), 539–552. https://doi.org/10.1080/10635150600755453

Bacal, S., Burduja, D., Buşmachiu, G., Cebotari, C. & Merkl, O. 2020. Longhorn beetles in the entomological collections of the Republic of Moldova (Coleoptera: Cerambycidae). *Folia Entomologica Hungarica*, **81**, 43–72. https://doi.org/10.17112/foliaenthung.2020.81.43

Bouckaert, R., Vaughan, T. G., Barido-Sottani, J., Duchêne, S., Fourment, M., Gavryushkina, A. et al. 2019. BEAST 2.5: An advanced software platform for Bayesian evolutionary analysis. *PLoS Computational Biology*, **15** (4), e1006650. https://doi.org/10.1371/journal.pcbi.1006650

Caba, F. & Dascălu, M. 2024. Dissecting natural hybridisation in longhorned beetles through an integrative approach: Further proof of reticulate evolution in Dorcadionini (Cerambycidae, Lamiinae). *Zoologica Scripta*, **53** (5), 665–687. https://doi.org/10.1111/zsc.12664

Council Directive 92/43/EEC. 1992. On the conservation of natural habitats and of wild fauna and flora. *Official Journal of the European Communities*, **L** (206), 7–50.

Council of Europe. 2011. *Revised Annex I of Resolution 6 of the Bern Convention listing the species requiring specific habitat conservation measures*.

Crișan, A., Manci, C.-O., Ruicănescu, A. & Rákosy, L. 2017. Information about the biology, ecology and distribution of *Pilemia tigrina* (Mulsant, 1851) in Romania (Coleoptera: Cerambycidae). *Entomologica Romanica*, **21**: 9–14. https://doi.org/10.24193/entomolrom.21.2

Dascălu, M.-M., Caba, F.-G. & Fusu, L. 2021. DNA barcoding in Dorcadionini (Coleoptera, Cerambycidae) uncovers mitochondrial-morphological discordance and the hybridogenic origin of several subspecies. *Organisms Diversity & Evolution*, **22**(1), 205–229. https://doi.org/10.1007/s13127-021-00531-x

Drummond, A.J., Ho, S.Y.W., Phillips, M.J. & Rambaut, A. 2006. Relaxed phylogenetics and dating with confidence. *PLoS Biology*, **4** (5), e88. https://doi.org/10.1371/journal.pbio.0040088

Eckert, C. G., Samis, K. E. & Lougheed, S. C. 2008. Genetic variation across species' geographical ranges: The central–marginal hypothesis and beyond. *Molecular Ecology*, **17** (5), 1170–1188. https://doi.org/10.1111/j.1365-294x.2007.03659.x

European Commission. 2018. *Report under Article 17 of the Habitats Directive (reporting period: 2013–2018). Pilemia tigrina assessments at EU biogeographical level.*

Gascuel, O. 1997. BIONJ: An improved version of the NJ algorithm based on a simple model of sequence data. *Molecular Biology and Evolution*, **14** (7), 685–695. https://doi.org/10.1093/oxfordjournals.molbev.a025808

Gernhard, T. 2008. The conditioned reconstructed process. *Journal of Theoretical Biology*, **253** (4), 769–778. https://doi.org/10.1016/j.jtbi.2008.04.005

Georgiev, G. 2020. New records of longhorn beetles (Coleoptera: Cerambycidae) in entomological collections in Bulgaria. *Forest Science*, **56** (1), 87–99.

Gouy, M., Tannier, E., Comte, N. & Parsons, D. P. 2021. Seaview Version 5: A multiplatform software for multiple sequence alignment, molecular phylogenetic analyses, and tree reconciliation. *Methods in Molecular Biology*, **2231**, 241–260. https://doi.org/10.1007/978-1-0716-1036-7_15

Guindon, S., Dufayard, J. F., Lefort, V., Anisimova, M., Hordijk, W. & Gascuel, O. 2010. New algorithms and methods to estimate maximum-likelihood phylogenies: Assessing the performance of PhyML 3.0. *Systematic Biology*, **59** (3), 307–321. https://doi.org/10.1093/sysbio/syq010

Hargreaves, A. L. & Eckert, C. G. 2013. Evolution of dispersal and mating systems along geographic gradients: Implications for shifting ranges. *Functional Ecology*, **28** (1), 5–21. https://doi.org/10.1111/1365-2435.12170

Ilić, N. & Ćurčić, S. 2015. A checklist of longhorn beetles (Coleoptera: Cerambycidae) of Serbia. *Zootaxa*, **4026** (1), 1–97. https://doi.org/10.11646/zootaxa.4026.1.1

Jukes, T. H. & Cantor, C. R. 1969. Evolution of Protein Molecules. *In*: Munro, H. N., ed. *Mammalian Protein Metabolism*. Academic Press, New York, 21–132.

Karpiński, L., Gorring, P. & Cognato, A. I. 2023. DNA vs. morphology in delineating species boundaries of endemic Mongolian *Eodorcadion* taxa (Coleoptera: Cerambycidae). *Diversity*, **15** (5), 662. https://doi.org/10.3390/d15050662

Karpiński, L., Gorring, P., Enkhnasan, D. & Cognato, A. I. 2024. First support for phylogenetically segregated ecotypes and delineating thresholds for inter- and intraspecific ranks in phytophagous Central Asian beetles (Coleoptera). *Zoologica Scripta*, **54** (2), 144–162. https://doi.org/10.1111/zsc.12702

Korlević, P., McAlister, E., Mayho, M., Makunin, A., Flicek, P. & Lawniczak, M. K. N. 2021. A minimally morphologically destructive approach for DNA retrieval and whole-genome shotgun sequencing of pinned historic Dipteran vector species. *Genome Biology and Evolution*, **13** (10).https://doi.org/10.1093/gbe/evab226

Makunin, A., Korlević, P., Park, N., Goodwin, S., Waterhouse, R. M., von Wyschetzki, K., Jacob, C. G., Davies, R., Kwiatkowski, D., St. Laurent, B., Ayala, D. & Lawniczak, M. K. N.

2022. A targeted amplicon sequencing panel to simultaneously identify mosquito species and *Plasmodium* presence across the entire *Anopheles* genus. *Molecular Ecology Resources*, **22** (1), 28–44. https://doi.org/10.1111/1755-0998.13436

Rambaut, A. 2014. FigTree v1.4.2, a graphical viewer of phylogenetic trees. Available at: http://tree.bio.ed.ac.uk/software/figtree/

Rambaut, A., Drummond, A. J., Xie, D., Baele, G. & Suchard, M. A. 2018. Posterior summarisation in Bayesian phylogenetics using Tracer 1.7. *Systematic Biology*, **67** (5), 901–904. https://doi.org/10.1093/sysbio/syy032

Scherrenberg, M. D. W., Berends, C. J., & van de Wal, R. S. W. 2025. CO_2 and summer insolation as drivers for the Mid-Pleistocene Transition. *Climate of the Past*, **21** (6), 1061–1077. https://doi.org/10.5194/cp-21-1061-2025

Srivathsan, A., Lee, L., Katoh, K., Hartop, E., Kutty, S. N., Wong, J., Yeo, D. & Meier, R. 2021. ONTbarcoder and MinION barcodes aid biodiversity discovery and identification by everyone, for everyone. *BMC Biology*, **19** (1). https://doi.org/10.1186/s12915-021-01141-x

Srivathsan, A., Feng, V., Suárez, D., Emerson, B. & Meier, R. 2024. ONTbarcoder 2.0: Rapid species discovery and identification with real-time barcoding facilitated by Oxford Nanopore R10.4. *Cladistics*, **40** (2), 192–203. https://doi.org/10.1111/cla.12566

Tezcan, S., Karsavuran, Y., Pehlivan, E. & Özdikmen, H. 2020. Catalogue of longhorned beetles of LEMT (Lodos Entomological Museum, Turkey) (Coleoptera: Cerambycidae) Part II: Lamiinae and Dorcadioninae. *Munis Entomology & Zoology*, **15**(1), 145–170.

Tóth, I.Z., Csathó, A. I., Buşmachiu, G. & Merkl, O. 2016. *Pilemia tigrina*: New and corrected records from the Republic of Moldova, Hungary and Romania (Coleoptera: Cerambycidae). *Folia Entomologica Hungarica*, **77**, 33–40. https://doi.org/10.17112/foliaenthung.2016.77.33

Turner, T. 2013. Faculty Opinions recommendation of Macroevolutionary speciation rates are decoupled from the evolution of intrinsic reproductive isolation in *Drosophila* and birds. [dataset]. *In*: *Faculty Opinions — Post-Publication Peer Review of the Biomedical Literature*. H1 Connect. https://doi.org/10.3410/f.718098614.793485011

Vitali, F. 2015. Saperdacaroli n. sp., a new fossil species from Early Eocene of Colorado, with taxonomic remarks on its extinct congeners (Coleoptera, Cerambycidae). *Les Cahiers Magellanes*, *Nouvelle Série*, 17, 20–28.

Zamoroka, A. M., Semaniuk, D. V., Shparyk, V. Yu. & Mykytyn, T. V. 2019. Taxonomic position of *Anastrangalia reyi* and *A. sequensi* (Coleoptera, Cerambycidae) based on molecular and morphological data. *Vestnik Zoologii*, **53** (3), 209–226. https://doi.org/10.2478/vzoo-2019-0021

Zamoroka, A. 2022 a. *Phytoecia* in Ukraine (Coleoptera: Cerambycidae). *In*: Myroniuk, I. S., Roshko, V. H., Hasynets, Ya. S. et al., eds. *Abstracts of International Scientific Conference* (Ukraine, Uzhhorod, 30 September–02 October, 2022). Uzhhorod: "Hoverla", 9–10.

Zamoroka, A. 2022 b. The longhorn beetles included in the Red Data Book of Ukraine, the fourth edition – data analysis. *In*: Yanytskyi, T. P. et al., eds. *Current Issues in the Study of the Entomofauna of the Western Region of Ukraine: Abstracts of the Scientific and Practical Conference "XVI Lviv Entomological School"* (Lviv, October 25, 2022). State Natural History Museum of the NAS of Ukraine, Lviv, 19–21 [In Ukrainian].

Zamoroka, A. M. 2022 c. The longhorn beetles (Coleoptera, Cerambycidae) of Ukraine: Results of two centuries of research. *Biosystem Diversity*, **30** (1), 46–74. https://doi.org/10.15421/012206

Zamoroka, A. M. 2022 d. Molecular revision of *Rhagiinisensu* lato (Coleoptera, Cerambycidae): Paraphyly, intricate evolution and novel taxonomy. *Biosystem Diversity*, **30** (3), 295–309. https://doi.org/10.15421/012232

Zamoroka, A. M., Tròcoli, S., Shparyk, V. Yu. & Semaniuk, D. V. 2022. Polyphyly of the genus *Stenurella* (Coleoptera, Cerambycidae): Consensus of morphological and molecular data. *Biosystem Diversity*, **30** (2), 119–136. https://doi.org/10.15421/012212

Zamoroka, A. M. 2023. New additions to the fauna of the longhorn beetles in Ukraine with a new record of rare, poorly known and invasive species. *Baltic Journal of Coleopterology*, **23** (2), 159–188. https://doi.org/10.59893/bjc.23(2).002

Zamoroka, A. M., Ruicănescu, A. & Manci, C.-O. 2024. East and West of the Carpathian Arc: Evidence of postglacial ecological and morphological divergence of *Phytoecia tigrina* metapopulations (Coleoptera, Cerambycidae). *Biosystem Diversity*, **32** (1), 12–29. https://doi.org/10.15421/012402

Received 25 March 2025
Accepted 21 October 2025